

## Boronyl Chemistry: The BO Group as a New Ligand in Gas-Phase Clusters and Synthetic Compounds

Hua-Jin Zhai,<sup>\*,†,‡</sup> Qiang Chen,<sup>†</sup> Hui Bai,<sup>†</sup> Si-Dian Li,<sup>\*,†</sup> and Lai-Sheng Wang<sup>\*,‡</sup>

<sup>†</sup>Nanocluster Laboratory, Institute of Molecular Science, Shanxi University, Taiyuan 030006, China

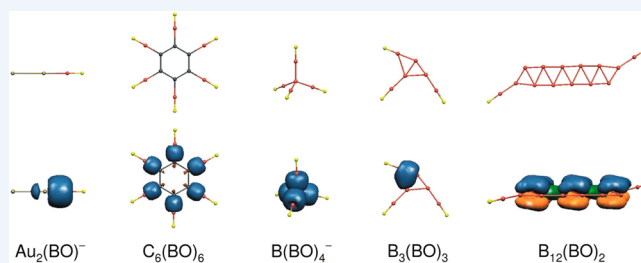
<sup>‡</sup>Department of Chemistry, Brown University, Providence, Rhode Island 02912, United States

**CONSPECTUS:** Boronyl (BO) is a monovalent  $\sigma$  radical with a robust B $\equiv$ O triple bond. Although BO/BO<sup>-</sup> are isoivalent to CN/CN<sup>-</sup> and CO, the chemistry of boronyl has remained relatively unknown until recently, whereas CN/CN<sup>-</sup> and CO are well-known inorganic ligands. Further analogy may be established for BO versus H or Au ligands, which are all monovalent  $\sigma$  radicals. This Account intends to provide an overview of research activities over the past few years that are relevant to the development of boronyl chemistry, in particular, in size-selected gaseous clusters containing BO.

The systems covered herein include transition metal boronyl clusters, carbon boronyl clusters, boron oxide clusters and boron boronyl complexes, the boronyl boroxine, and the first synthetic Pt–BO bulk compound. In these boronyl clusters and compounds, the BO groups show remarkable structural and chemical integrity as a ligand.

Among transition metal boronyls, gold monoboronyl clusters Au<sub>n</sub>(BO)<sup>-</sup> and Au<sub>n</sub>(BO) ( $n = 1-3$ ) have been characterized, and they are shown to possess electronic and structural properties similar to the corresponding Au<sub>n+1</sub><sup>-</sup> and Au<sub>n+1</sub> bare clusters, demonstrating the BO/Au analogy. The Au–B bonding in the Au–BO clusters is highly covalent. A recent advance in boronyl chemistry is the successful synthesis and isolation of the first boronyl compound, *trans*-[(Cy<sub>3</sub>P)<sub>2</sub>BrPt(BO)]. This unique Pt–BO compound and other potential transition metal boronyl compounds may find applications in catalysis and as chemical building blocks. Carbon boronyl clusters versus boron carbonyl clusters is a topic of interest in designing new aromatic complexes. Experimental and theoretical data obtained to date show that carbon boronyl clusters are generally far more stable than their boron carbonyl counterparts, highlighting the potency of boronyl as a ligand in aromatic compounds. Notably, in light of the BO/H analogy, the perfectly hexagonal (CBO)<sub>6</sub> cluster is a carbon boronyl analogue of benzene.

The BO groups also dominate the structures and bonding of boron oxide clusters and boron boronyl complexes, in which BO groups occupy terminal, bridging, or face-capping positions. The bridging  $\eta^2$ -BO groups feature three-center two-electron bonds, akin to the BHB  $\tau$  bonds in boranes. A close isolobal analogy is thus established between boron oxide clusters and boranes, offering vast opportunities for the rational design of novel boron oxide clusters and compounds. Boron boronyl clusters may also serve as molecular models for mechanistic understanding of the combustion of boron and boranes. An effort to tune the B versus O composition in boron oxide clusters leads to the discovery of boronyl boroxine, *D*<sub>3h</sub> B<sub>3</sub>O<sub>3</sub>(BO)<sub>3</sub>, an analogue of boroxine and borazine and a new member of the “inorganic benzene” family. Furthermore, a unique concept of  $\pi$  and  $\sigma$  double conjugation is proposed for the first time to elucidate the structures and bonding in the double-chain nanoribbon boron diboronyl clusters, which appear to be inorganic analogues of polyenes, cumulenes, and polynes. This Account concludes with a brief outlook for the future directions in this emerging and expanding research field.



### 1. INTRODUCTION

Boron possesses unique structural and bonding properties and has a rich chemistry second only to carbon. Elemental boron and boron compounds show vast structural diversity, featuring icosahedral B<sub>12</sub> cages as the key structural units.<sup>1</sup> The chemistry of boron, such as that of boranes,<sup>2</sup> is also dominated by the three-dimensional cage molecules. Due to the intrinsic electron deficiency of boron, the bonding in boranes is elucidated via the concept of three-center two-electron (3c–2e) bond, which has been a cornerstone in modern chemical bonding theory. In stark contrast, joint experimental and theoretical investigations over the past decade have shown that size-selected boron clusters possess planar or quasi-planar structures in a wide size

range.<sup>3–12</sup> The flat world of boron is governed by aromaticity and antiaromaticity, bearing interesting resemblance to aromatic hydrocarbons.<sup>3,4,6–11,13–15</sup>

Boron is also known for its oxygen affinity and the combustion of boron and boranes has received persistent interest since the 1950s, primarily aimed at the development of highly energetic boron-based propellants.<sup>16</sup> Boronyl (BO)<sup>17,18</sup> possesses a strong triple bond between boron and oxygen, with BO/BO<sup>-</sup> being isoivalent to CN/CN<sup>-</sup> and CO. However, the chemistry of boronyl has remained relatively unknown, whereas

Received: March 28, 2014

Published: June 10, 2014

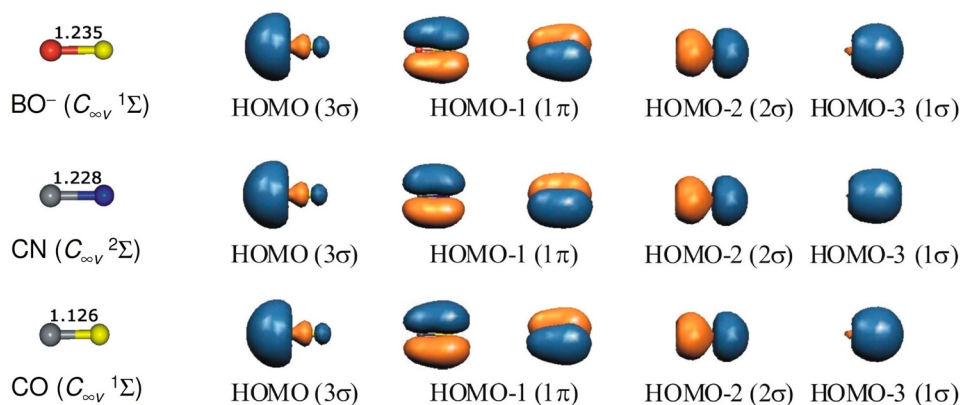


**Figure 1.** Comparison of bond distances (in Å) and molecular orbitals of  $\text{BO}^-$ , CN, and CO.

CN and CO are well-known inorganic ligands. An early claim of the synthesis of boranilide ( $\text{C}_6\text{H}_5$ ) $\text{NH}(\text{BO})$  dated back to 1920, but it was later disputed to be actually the double salt of aniline and zinc chloride.<sup>19</sup> An experimental study on liquid  $\text{B}_2\text{O}_3$  in 1959 led to the hypothesis that BO groups are formed as termini of the continuous network in the liquid with increasing temperature.<sup>20</sup> In 1988, gas-phase boron oxide cation clusters<sup>21</sup> were produced from vitreous boron trioxide, whose “guess” structures are built on integral  $\text{BO}_3$  triangles with branches terminated by BO groups. The methylboron oxide molecule,  $\text{H}_3\text{C}(\text{BO})$ , was characterized in 1989 using photoelectron spectroscopy (PES), and comparisons with isovalent  $\text{H}_3\text{C}(\text{CN})$  species allowed the assignment of the  $\text{B}\equiv\text{O}$  triple bond.<sup>22</sup> Even though the PES spectrum of  $\text{BO}^-$  was reported in 1997,<sup>17</sup> systematic spectroscopic studies of boron oxide clusters and boronyl complexes started in 2007 when laser vaporization was used to produce the related boronyl complexes in combination with the magnetic-bottle PES technique.<sup>17,23</sup>

The past few years have witnessed increasing experimental and computational efforts in the development of boronyl chemistry, from gas-phase clusters to synthetic compounds. These studies span a range of systems, including transition metal boronyl clusters,<sup>24,25</sup> carbon boronyl clusters,<sup>22,26–31</sup> boron oxide clusters and boron boronyl complexes,<sup>17,18,32–45</sup> boronyl boroxine,<sup>46</sup> and the synthesis of the first Pt–BO bulk compound.<sup>47</sup> In all boronyl clusters and compounds, the BO group demonstrates structural and chemical robustness, suggesting promising opportunities for the development of boronyl chemistry that is comparable to those of CN or CO. A large body of the experimental studies are accomplished using the anion PES technique,<sup>23,24,32–37,39</sup> which accesses the ground state and excited states of a neutral species and provides electronic and structural information for both anion and neutral clusters. In this Account, we attempt to provide a brief overview of this emerging field.

## 2. BORONYL AS A MONOVALENT $\sigma$ LIGAND: $\text{BO}/\text{BO}^-$ VERSUS $\text{CN}/\text{CN}^-$ AND CO

The bonding in  $\text{BO}/\text{BO}^-$  was analyzed recently (Figure 1).<sup>17,18</sup> The  $1\sigma$  HOMO – 3, where HOMO denotes the highest occupied molecular orbital, of  $\text{BO}^-$  is an O 2s lone pair. HOMO – 2 is a  $\sigma$  bonding orbital with mixed covalent and ionic characters, mainly composed of O 2p and B 2s atomic orbitals (AOs). The degenerate HOMO – 1 orbitals are  $\pi$  bonding, involving B 2p and O 2p AOs. The HOMO is primarily composed of B 2s AOs with slight antibonding

character. The same bonding pattern holds for BO except that only one electron is filled in the HOMO, rendering it a monovalent  $\sigma$  radical. Both BO and  $\text{BO}^-$  can be viewed as a triple bond, consistent with their short bond distances of 1.203 and 1.235 Å, respectively, at the B3LYP/aug-cc-pVTZ level.<sup>18</sup> Overall,  $\text{BO}/\text{BO}^-$  share the same bonding pattern as  $\text{CN}/\text{CN}^-$  and CO. However, the ground-state electron binding energies differ: 2.51 eV for  $\text{BO}^-$  versus 3.86 eV for  $\text{CN}^-$  and 14.99 eV for CO. In terms of the bond strength, BO is comparable to and actually stronger than CN (CO 1076 kJ/mol; BO 806 kJ/mol; and CN 770 kJ/mol). Thus, BO and  $\text{BO}^-$  are rather robust species and may serve as effective ligands and retain their integrity in compounds.

## 3. METAL BORONYLS

### 3.1. Au–BO Clusters

While working on Au–B alloy clusters, an auroboron oxide cluster,  $\text{Au}_2(\text{BO})^-$ , was observed as a predominant peak in the Au–B mass spectrum,<sup>24</sup> hinting at a highly stable anion. The PES spectra of  $\text{Au}_n(\text{BO})^-$  ( $n = 1–3$ ) exhibit an even–odd alternation in adiabatic detachment energies (ADEs): 1.46, 4.32, and 3.08 eV, respectively, which are also the electron affinities (EAs) of the corresponding neutral species. The EA of  $\text{Au}_2(\text{BO})$  is extremely high, which underlies its dominance in the mass spectrum, rendering it a superhalogen species. The PES spectra of  $\text{Au}(\text{BO})^-$  and  $\text{Au}_3(\text{BO})^-$  each exhibit a huge energy gap, 3.27 and 1.83 eV, respectively, between the ground state X and the first excited state A, suggesting closed-shell neutral clusters with large gaps between the HOMO and the lowest unoccupied molecular orbital (LUMO). These observations are in line with those for bare  $\text{Au}_{n+1}^-$  ( $n = 1–3$ ) clusters (EAs 2.01 eV for  $\text{Au}_2$ , 3.88 eV for  $\text{Au}_3$ , and 2.75 eV for  $\text{Au}_4$ ; energy gaps 2.00 eV for  $\text{Au}_2^-$  and 1.57 eV for  $\text{Au}_4^-$ ),<sup>48</sup> hinting that the BO group in  $\text{Au}_n(\text{BO})^-$  ( $n = 1–3$ ) is equivalent to a Au atom in  $\text{Au}_{n+1}^-$ , which are both monovalent  $\sigma$  ligands. This concept was further tested in the  $\text{B}_{10}(\text{BO})^-$  and  $\text{B}_{12}(\text{BO})^-$  clusters, which are isovalent to  $\text{B}_{10}\text{Au}^-$  and  $\text{B}_{12}\text{Au}^-$ , respectively.<sup>34,36</sup>

Cluster structures of  $\text{Au}_n(\text{BO})^-$  ( $n = 1–3$ ) are depicted in Figure 2.<sup>24</sup>  $\text{Au}(\text{BO})^-$  and  $\text{Au}_2(\text{BO})^-$  are perfectly linear, similar to  $\text{Au}_2^-$  and  $\text{Au}_3^-$  by replacing one Au atom with a terminal BO group. Two isomers coexist for  $\text{Au}_3(\text{BO})^-$ , where the  $C_s$  isomer (quasi-linear) is slightly higher in energy than the  $C_{2v}$  isomer (Y-shaped). Both isomers were also observed for  $\text{Au}_4^-$ .<sup>48</sup> Remarkably, the  $\text{B}\equiv\text{O}$  bond distances (1.219–1.225 Å) in  $\text{Au}_n(\text{BO})^-$  ( $n = 1–3$ ) are close to that of the gas-phase BO

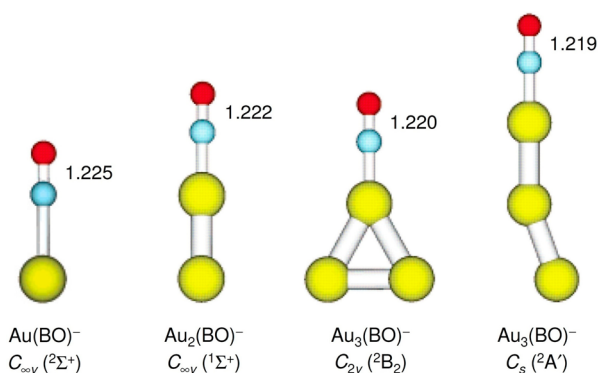


**Figure 2.** Optimized structures of  $\text{Au}_n(\text{BO})^-$  ( $n = 1-3$ ) at the B3LYP level. The  $\text{B}=\text{O}$  bond distances (in Å) are labeled. Reproduced with permission from ref 24. Copyright 2007 American Chemical Society.

molecule (B3LYP, 1.203 Å),<sup>18</sup> highlighting the robustness of BO group as a  $\sigma$  radical in the Au–BO complexes. A subsequent theoretical work<sup>25</sup> showed that the Au–B bonding in  $\text{Au}(\text{BO})_2^-$  is more covalent relative to the isovalent  $\text{Au}(\text{CN})_2^-$  species. Covalent Au–B bonding was also discussed in other Au–B alloy clusters, such as  $\text{B}_7\text{Au}_2^-$ ,  $\text{B}_{10}\text{Au}^-$ , and  $\text{B}_{12}\text{Au}^-$ .<sup>34,36,49</sup>

### 3.2. The First *trans*-[( $\text{Cy}_3\text{P}$ )<sub>2</sub>BrPt(BO)] Synthetic Compound

Very recently, the first platinum boronyl compound, *trans*-[( $\text{Cy}_3\text{P}$ )<sub>2</sub>BrPt(BO)], was successfully synthesized and isolated (Figure 3)<sup>47</sup> by taking advantage of a unique approach of

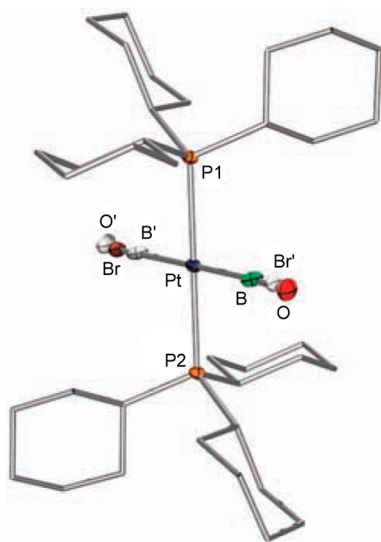


**Figure 3.** Molecular structure of *trans*-[( $\text{Cy}_3\text{P}$ )<sub>2</sub>BrPt(BO)] as revealed from single-crystal X-ray diffraction, showing a BO ligand coordinating terminally via B to the Pt center. The  $\text{B}=\text{O}$  linkage is further characterized by infrared spectroscopy. Reproduced with permission from ref 47. Copyright 2010 The American Association for the Advancement of Science.

generating unusual ligand systems in the coordination sphere of transition metals. The compound is inert toward oligomerization and exhibits good thermal and light stability. The BO group is coordinated to Pt in a terminal fashion. The bonding interactions can be described essentially as two  $\pi$  bonds with stabilizing contributions of the symmetry-equivalent d-orbitals of Pt. The BO bond distance was determined to be 1.205 Å, which is consistent with a triple bond and again comparable to

the gas-phase BO molecule (B3LYP 1.203 Å).<sup>18</sup> The assigned BO stretching frequencies in the infrared spectroscopy, 1853/1797  $\text{cm}^{-1}$  for the two boron isotopologues,<sup>47</sup> appear to be smaller than those of the gas-phase BO cluster (1935/1886  $\text{cm}^{-1}$ , respectively),<sup>18</sup> akin to the red-shifting of the stretching frequencies in metal carbonyls relative to the free CO molecule. However, it is unclear how BO acts as a  $\pi$  acceptor ligand compared with CO and CN, which requires further experimental and computational characterizations. The Pt–BO compound may find useful applications as chemical building blocks and in catalysis.

## 4. CARBON BORONYLS

### 4.1. $\text{H}_3\text{C}(\text{BO})$ : Methylboron Oxide

By pyrolysis of 2-methyl-1,3,2-dioxaborolane-4,5-dione, the methylboron oxide molecule,  $\text{H}_3\text{C}(\text{BO})$ , was generated, and its radical cation states were probed via PES experiment with the aid of theoretical calculations.<sup>22</sup> Methylboron oxide is a derivative of methane. The PES of  $\text{H}_3\text{C}(\text{BO})$  was shown to bear similarity to that of the well-known isovalent  $\text{H}_3\text{C}(\text{CN})$  species. This spectroscopic observation provides early clues that the BO group possesses a  $\text{B}=\text{O}$  triple bond, akin to  $\text{C}\equiv\text{N}$ . The optimized BO bond distance in  $\text{H}_3\text{C}(\text{BO})$  at the Hartree–Fock level is 1.216 Å, close to the gas-phase BO radical (B3LYP, 1.203 Å).<sup>18</sup> The thermodynamic stability of  $\text{H}_3\text{C}(\text{BO})$  suggests the possibility to isolate derivatives of organoboron oxides with bulky alkyl or aryl groups. Similarly, by BO/H substitution in hydrocarbons, isovalent molecules that contain BO groups, such as  $\text{C}_2\text{H}_{4-m}(\text{BO})_m$  ( $m = 1-4$ ),  $\text{C}_2\text{H}_{2-m}(\text{BO})_m$  ( $m = 1, 2$ ),  $\text{B}_n(\text{BO})_n^{2-}$ ,  $\text{CB}_{n-1}(\text{BO})_n^-$ , and  $\text{C}_2\text{B}_{n-2}(\text{BO})_n$  ( $n = 5-12$ ), were pursued computationally.<sup>28,29</sup> The viability of these complexes remains to be tested experimentally.

### 4.2. (OC)BB(CO), (OB)BC(CO), and (OB)CC(BO) Clusters

In a low temperature matrix infrared spectroscopic study,<sup>50</sup> a linear (OC)BB(CO) cluster was identified, in which two CO groups are attached terminally to the BB core, featuring “some”  $\text{B}=\text{B}$  triple bond character. However, a subsequent work<sup>26</sup> showed that (OC)BB(CO) is highly unstable on its potential energy surface, readily undergoing photochemical rearrangements (photoinduced isomerization) to successively form (OB)BC(CO) and (OB)CC(BO). The latter species are  $\sim 2.6$  and  $\sim 4.1$  eV more stable at B3LYP level, respectively. The exact mechanism for such isomerization is unclear. Nonetheless, the studies hint that boronyl species can be more stable than their corresponding carbonyls. It is stressed that the (OC)BB(CO) cluster is only a local minimum and, therefore, strategies (such as ligand replacement) need to be designed to further stabilize the  $\text{B}=\text{B}$  core in order to pursue its bulk synthesis.

### 4.3. Carbon Boronyls versus Boron Carbonyls

In an effort to design new aromatic compounds based on prototypical aromatic hydrocarbons, monocyclic boron carbonyl clusters  $(\text{BCO})_n$  ( $n = 3-7$ ) were initially proposed computationally.<sup>51</sup> Further work<sup>27</sup> showed that the monocyclic carbon boronyl clusters are thermodynamically much more stable, with the  $(\text{CBO})_2$ ,  $(\text{CBO})_3^+$ ,  $(\text{CBO})_4^{2-}$ ,  $(\text{CBO})_5^-$ ,  $(\text{CBO})_6$ , and  $(\text{CBO})_7^-$  clusters being 4.15, 1.61, 8.01, 10.36, 9.26, and 5.97 eV lower in energy than their  $(\text{BCO})_n$  counterparts, respectively, at B3LYP level. Considering the fact of BO/H analogy, the  $(\text{CBO})_n$  ( $n = 3-7$ ) clusters are actually boronyl analogues of hydrocarbon molecules  $(\text{CH})_n$ .

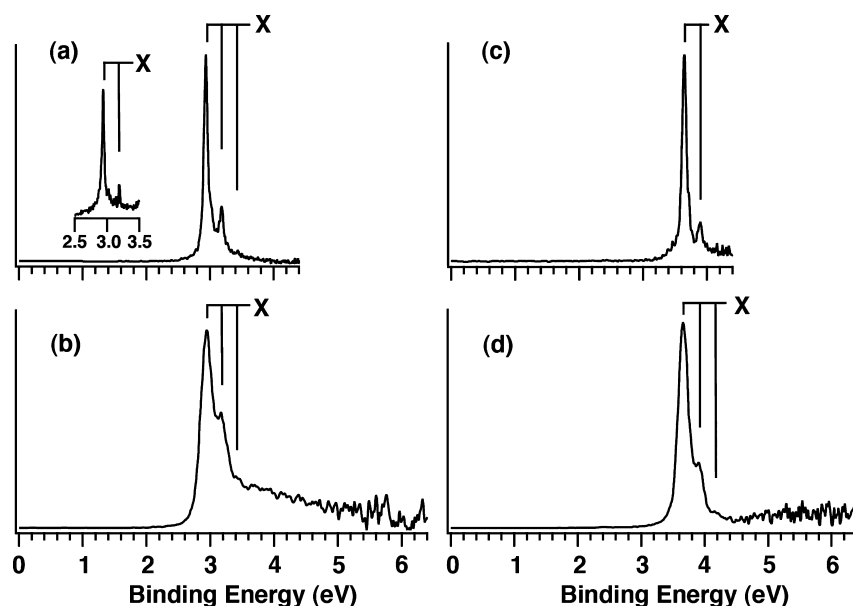


**Figure 4.** Photoelectron spectra of  $\text{B}_3\text{O}_2^-$  at (a) 266 nm and (b) 193 nm, and of  $\text{B}_4\text{O}_3^-$  at (c) 266 nm and (d) 193 nm. The inset in part a shows the 355 nm spectrum. Vertical lines represent vibrational structures. Reproduced with permission from ref 32. Copyright 2007 American Chemical Society.

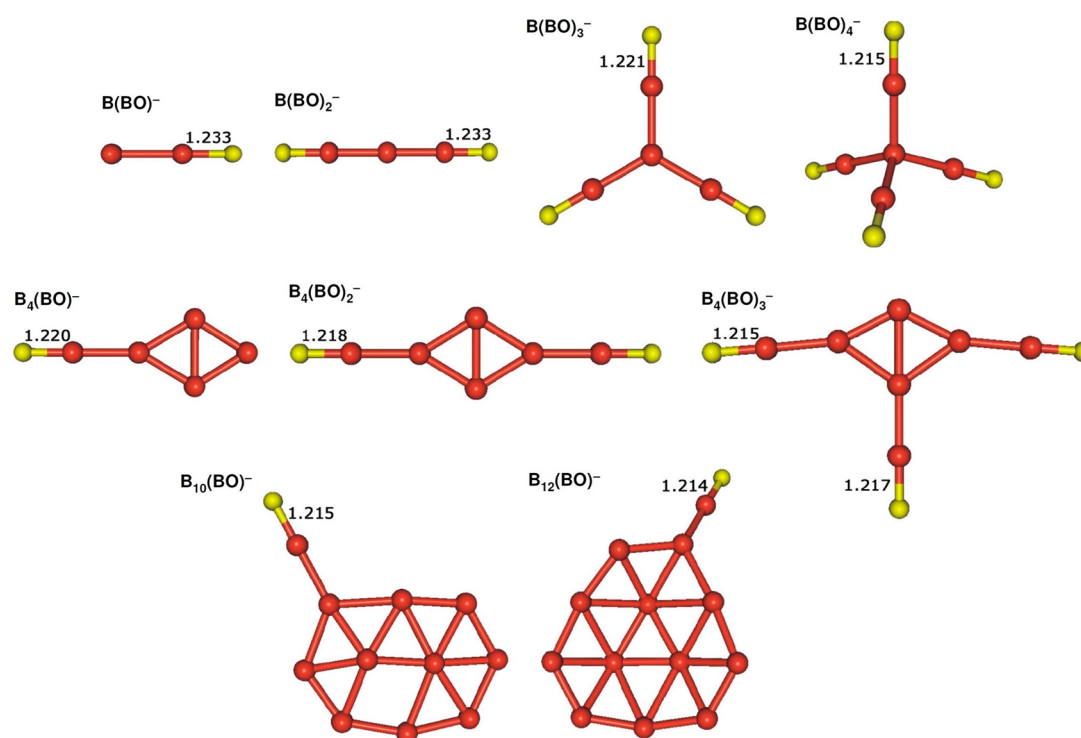


**Figure 5.** Optimized global-minimum structures<sup>32,34–36,40</sup> at the B3LYP/aug-cc-pVTZ level for  $\text{B}(\text{BO})_n^-$  ( $n = 1-4$ ),  $\text{B}_4(\text{BO})_n^-$  ( $n = 1-3$ ),  $\text{B}_{10}(\text{BO})^-$ , and  $\text{B}_{12}(\text{BO})^-$ . The  $\text{B}\equiv\text{O}$  bond distances (in Å) are labeled.

For example, the perfectly hexagonal aromatic  $(\text{CBO})_6$  cluster is the carbon boronyl analogue of benzene.

## 5. BORON BORONYLS AND BORONYL BOROXINE

### 5.1. Boronyl as a Terminal Ligand and Analogy between Boron Oxide Clusters and Boranes

Recent PES<sup>17,18,32–37,39</sup> and computational<sup>38,40–44</sup> studies have characterized a variety of boron oxide clusters, which can be faithfully classified as boron boronyl clusters. Figure 4 shows

the PES spectra of  $\text{B}_3\text{O}_2^-$  and  $\text{B}_4\text{O}_3^-$ .<sup>32</sup> The similar and surprisingly simple PES spectra exhibit well-resolved vibrational structures of  $1950\text{ cm}^{-1}$  for  $\text{B}_3\text{O}_2$  and  $1980\text{ cm}^{-1}$  for  $\text{B}_4\text{O}_3$  due to symmetric  $\text{B}\equiv\text{O}$  stretching (enriched  $^{10}\text{B}$  target used), consistent with the identified global-minimum structures:  $\text{B}(\text{BO})_2^-$  ( $D_{\infty h}$ ,  $^3\Sigma_g^-$ ),  $\text{B}(\text{BO})_2$  ( $D_{\infty h}$ ,  $^2\Pi_u$ ),  $\text{B}(\text{BO})_3^-$  ( $D_{3h}$ ,  $^2A_2''$ ), and  $\text{B}(\text{BO})_3$  ( $D_{3h}$ ,  $^1A_1'$ ). A selected set of boron boronyl clusters are depicted in Figure 5, including  $\text{B}(\text{BO})_n^-$  ( $n = 1-4$ ),  $\text{B}_4(\text{BO})_n^-$  ( $n = 1-3$ ),  $\text{B}_{10}(\text{BO})^-$ , and  $\text{B}_{12}(\text{BO})^-$ , which are all



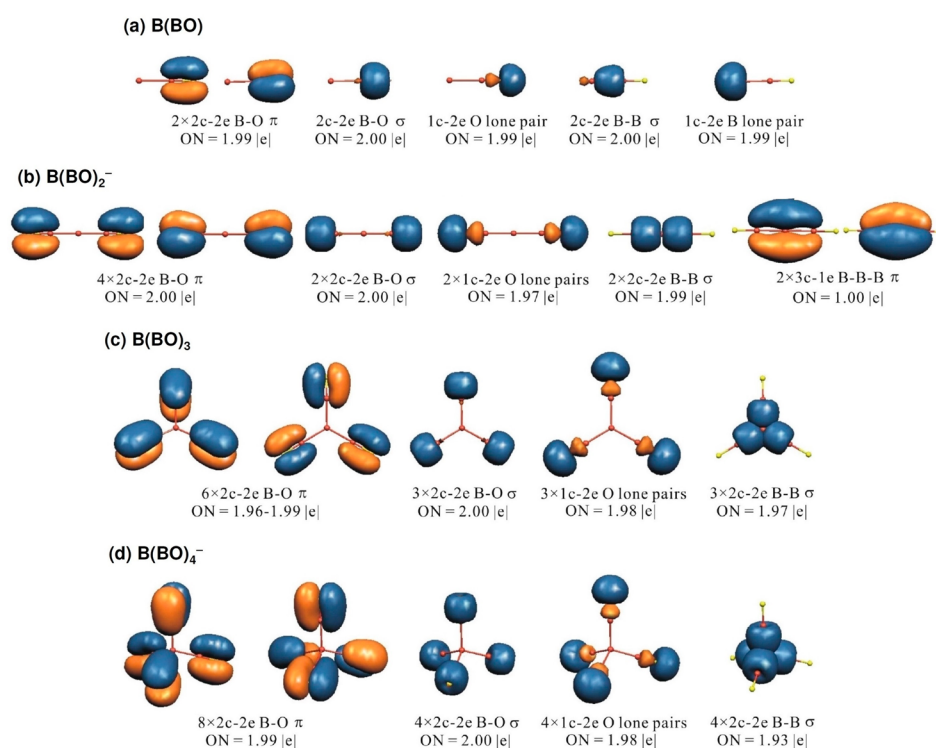


**Figure 6.** Bonding elements as revealed from the adaptive natural density partitioning (AdNDP) analyses for (a)  $B(BO)$ , (b)  $B(BO)_2^-$ , (c)  $B(BO)_3$ , and (d)  $B(BO)_4^-$ . Occupation numbers (ONs) are labeled.

global-minimum structures.<sup>32,34–36,40</sup> The latter two species are isostructural and isovalent to  $B_{10}Au^-$  and  $B_{12}Au^-$ , respectively, providing new examples for the BO/Au analogy.<sup>34,36</sup> It is immediately clear that a specific boron-rich  $B_mO_n^-/B_mO_n$  cluster can generally be formulated as  $B_{m-n}(BO)_n^-/B_{m-n}(BO)_n$ , which is dominated entirely by the terminal BO groups and shows little structural resemblance to the bare  $B_m^-/B_m$  species.<sup>3–15</sup> Notably, the integrity of the BO group is maintained in the boron boronyl complexes ( $B \equiv O$  bond distances, 1.214–1.233 Å).

The  $B(BO)_n^-/B(BO)_n$  ( $n = 1-4$ ) clusters form a complete series,<sup>32,40</sup> whose bonding is analyzed via adaptive natural density partitioning (AdNDP).<sup>52</sup> In the AdNDP analysis, which is currently applicable only to closed-shell species, the bonding of a molecule is represented in terms of  $n$ -center two-electron ( $nc-2e$ ) bonds, where the  $n$  value ranges from one to the total number of atoms in the molecule. AdNDP thus recovers the classical Lewis bonding elements (lone pairs and  $2c-2e$  bonds), as well as the nonclassical  $nc-2e$  delocalized bonds. Clearly, the BO group maintains its triple bond nature (first three bonding elements in each panel; Figure 6) and the link between the B core and each BO group is classified as a single  $\sigma$  bond (the fifth bonding elements in each panel; Figure 6). Since BO is a monovalent  $\sigma$  radical akin to H, the  $B(BO)_n^-/B(BO)_n$  ( $n = 1-4$ ) species are boronyl analogues of the simplest boranes:  $BH_n^-/BH_n$  ( $n = 1-4$ ). Interestingly, the  $T_d$   $B(BO)_4^-$  cluster<sup>40</sup> is the global minimum of  $B_5O_4^-$ . The CCSD(T) single-point calculations predicted an extremely high EA of 6.94 eV for  $B(BO)_4$ , consistent with a stable, closed-shell  $B(BO)_4^-$  anion, similar to the isovalent  $BH_4^-$  or  $CH_4$  species.

## 5.2. The $(OB)BB(BO)^{2-}$ Dianion: Diboronyl Diborene with a $B \equiv B$ Triple Bond

B–B multiple bonds are rare due to boron’s electron deficiency. Evidence for “some”  $B \equiv B$  triple bond character was first reported for  $(OC)BB(CO)$  in matrix isolation spectroscopy (see section 4.2),<sup>26</sup> which is a local-minimum structure for the system. The  $(OB)BB(BO)^{0/-/2-}$  clusters are interesting species in terms of the B–B multiple bonds,<sup>33</sup> where the diboronyl diborene  $(OB)BB(BO)^{2-}$  dianion is isovalent to  $(OC)BB(CO)$  or  $(OB)CC(BO)$ . Experimentally, the PES spectra of  $B_4O_2^-$  reveal well-resolved vibrational structures with three modes for the ground-state transition X (Figure 7), consistent with the highly symmetric  $(OB)BB(BO)$  and  $(OB)BB(BO)^-$  clusters. These two clusters, along with their  $(OB)BB(BO)^{2-}$  dianion, all adopt perfectly linear geometries with two boronyl groups attached terminally to a  $B_2$  core, which represent true global-minimum structures (Figure 8a) on their potential energy surfaces.

In the  $(OB)BB(BO)^{0/-/2-}$  clusters, the bonding in the  $B_2$  core involves one  $\sigma$  orbital (fully occupied) and two  $\pi$  orbitals. Upon changing the charge state, the  $\pi$  orbitals are occupied by two to four electrons, which results in  $^3\Sigma_g^+$ ,  $^2\Pi_u$ , and  $^1\Sigma_g^+$  ground states with formal BB bond orders of 2, 2.5, and 3, respectively, the latter being the first global-minimum cluster with a  $B \equiv B$  triple bond. For the triplet  $(OB)BB(BO)$  neutral cluster with the Lewis structure of  $O \equiv B-B=B-B \equiv O$ , there are three totally symmetric stretching modes in its ground state. These modes are responsible for the observed vibrational structures:  $B \equiv O$  ( $2040 \pm 30$   $cm^{-1}$ ; enriched  $^{10}B$  target used),  $B \equiv B$  ( $1530 \pm 30$   $cm^{-1}$ ), and  $B-B$  ( $350 \pm 40$   $cm^{-1}$ ), thus providing valuable and definitive structural information.

Since the  $B_2(BO)_2^{2-}$  dianion is electronically unstable due to intramolecular Coulomb repulsion, a salt complex,  $B_2(BO)_2Li_2$ , was designed computationally (Figure 8b), whose isovalent

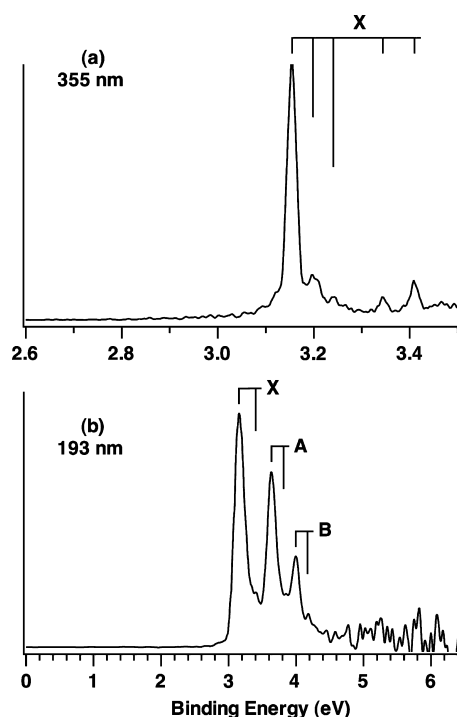


**Figure 7.** Photoelectron spectra of the  $B_4O_2^-$  cluster at (a) 355 nm and (b) 193 nm. The vertical lines represent vibrational structures. Reproduced with permission from ref 33. Copyright 2008 American Chemical Society.

$B_2H_2Li_2$  salt complex has two near degenerate structures ( $C_{2v}$  versus  $D_{2h}$ ; Figure 8c). The dianion and its salt complexes are isovalent to  $B_2H_2^{2-}$  (Figure 8d) and  $C_2H_2$  (Figure 8e), which also have a core  $B\equiv B$  or  $C\equiv C$  triple bond. Not surprisingly, the central BB bond distances in  $B_2(BO)_2$  (1.514 Å),  $B_2(BO)_2^-$  (1.482 Å), and  $B_2(BO)_2Li_2$  (1.455 Å) correlate closely with their bond orders. On the other hand, the terminal BO groups possess nearly constant bond distances (1.206–1.224 Å), comparable to the free BO molecule (1.203 Å).<sup>18</sup> Shortly after this work, a diboryne compound with a  $B\equiv B$  triple bond was synthesized in the bulk,<sup>53</sup> whose bond distance (1.449 Å) is in agreement with that in the  $B_2(BO)_2Li_2$  salt complex.

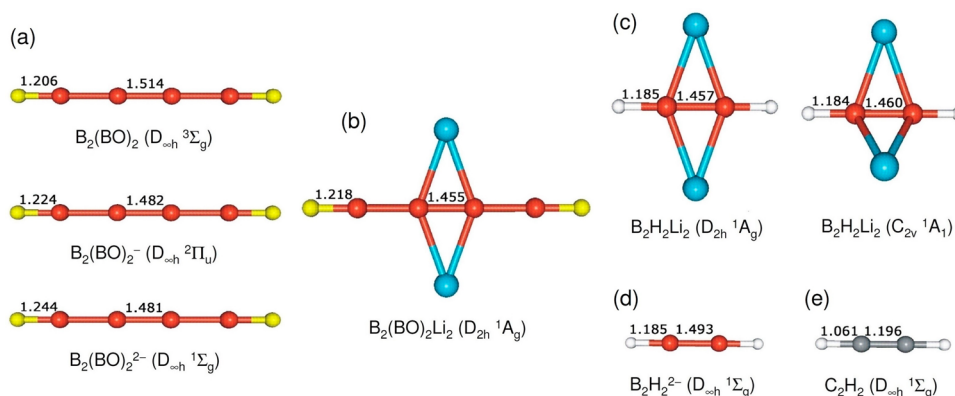


**Figure 8.** Optimized global-minimum structures at the B3LYP/aug-cc-pVTZ level for (a)  $B_2(BO)_2^{0/-/2-}$ , (b)  $B_2(BO)_2Li_2$  salt complex, (c)  $B_2H_2Li_2$  salt complex, (d)  $B_2H_2^{2-}$ , and (e)  $C_2H_2$ . The  $B\equiv O$ ,  $B-H$ , and central  $BB$  bond distances (in Å) are labeled. Reproduced with permission based on ref 33. Copyright 2008 American Chemical Society.

### 5.3. Boronyl as $\eta^2$ Bridging or $\mu^3$ Face-Capping Ligands

The celebrated  $3c-2e$  BHB bond is essential in the bonding in boranes.<sup>2</sup> For boron oxide clusters, the simplest  $3c-2e$   $\eta^2$  bridging  $B-(BO)-B$  bonds were observed in  $B_5O_3^-$  and  $B_6O_3^-$  (Figure 9).<sup>37</sup> Both clusters possess high electron binding energies (EAs: 4.34 eV for  $B_5O_3^-$  and 4.22 eV for  $B_6O_3^-$ ). A sizable energy gap of  $\sim 2$  eV was also observed for  $B_5O_3^-$ . The PES data facilitate the formulation of these clusters as  $B_2(BO)_3^-$  and  $B_3(BO)_3^-$ . Their global-minimum structures are  $C_{2v}$  ( $^1A_1$ ) and  $C_s$  ( $^2A'$ ), respectively (Figure 10), whose  $\eta^2$ -BO bridge group is reminiscent of the  $\eta^2$ -H bridge atom in boranes.

AdNDP analyses showed four delocalized electrons in  $B_2(BO)_3^-$ , which form one  $3c-2e$   $\pi$  bond and one bridging  $3c-2e$   $\eta^2$ -bond, the latter being analogous to the  $3c-2e$  BHB bond in boranes (Figure 10d). These delocalized bonds render double ( $\pi$  and  $\sigma$ ) aromaticity for  $B_2(BO)_3^-$ , demonstrating the bonding capability of  $\eta^2$ -BO bridge as a  $\sigma$  radical and a secondary  $\pi$  radical. There exists no such delocalized  $3c-2e$   $\pi$  system in  $C_{2v}$   $B_2H_3^-$ . For  $B_3(BO)_3$  neutral cluster, three pairs of delocalized electrons were revealed: one  $3c-2e$   $\sigma$  bond between the  $B\equiv O$  bridge and  $B_3$  core, one  $3c-2e$   $\sigma$  bond over the  $B_3$  core, and one  $4c-2e$   $\pi$  bond over four B atoms (Figure 10e). The  $4c-2e$   $\pi$  bond again demonstrates the  $\pi$ -bonding capability of  $\eta^2$ -BO bridge in addition to its  $\sigma$ -bonding ability. The observation of bridging  $\eta^2$ -BO group in  $B_2(BO)_3^-$  and  $B_3(BO)_3^-$  further establishes the isolobal analogy between boron oxide clusters and boranes. Recent theoretical works show that the face-capping  $\mu^3$  boronyl group<sup>38</sup> is also viable in complexes such as  $B_6(BO)_7^-$  (Figure 10c), as is the core boronyl group in small boron oxide clusters.<sup>54</sup> The  $B\equiv O$  bond distances in  $B_6(BO)_7^-$  vary slightly from terminal (1.206–1.208 Å) to face-capping (1.217 Å), similar to the behaviors of the CO ligand.

### 5.4. Boronyl Boroxine

Our recent computational structural searches revealed a perfectly planar  $D_{3h}$   $B_6O_6$  ( $^1A_1'$ ) cluster as the global minimum of the system,<sup>46</sup> which lies at least  $\sim 20$  kcal/mol lower in energy than alternative structures. It can be formulated as  $B_3O_3(BO)_3$  and features a boroxol  $B_3O_3$  ring as the core with three boronyl groups attached terminally, closely resembling boroxine and obtainable from the latter via isovalent BO/H substitution. Bonding analyses show weak  $\pi$  aromaticity in

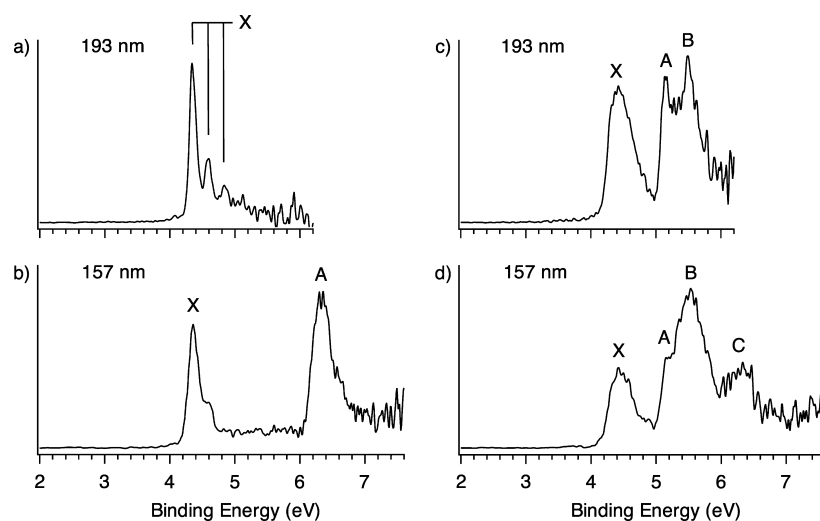


**Figure 9.** Photoelectron spectra of  $B_3O_3^-$  at (a) 193 nm and (b) 157 nm and of  $B_6O_3^-$  at (c) 193 nm and (d) 157 nm. The vertical lines represent vibrational structures. Reproduced with permission from ref 37. Copyright 2011 Wiley.

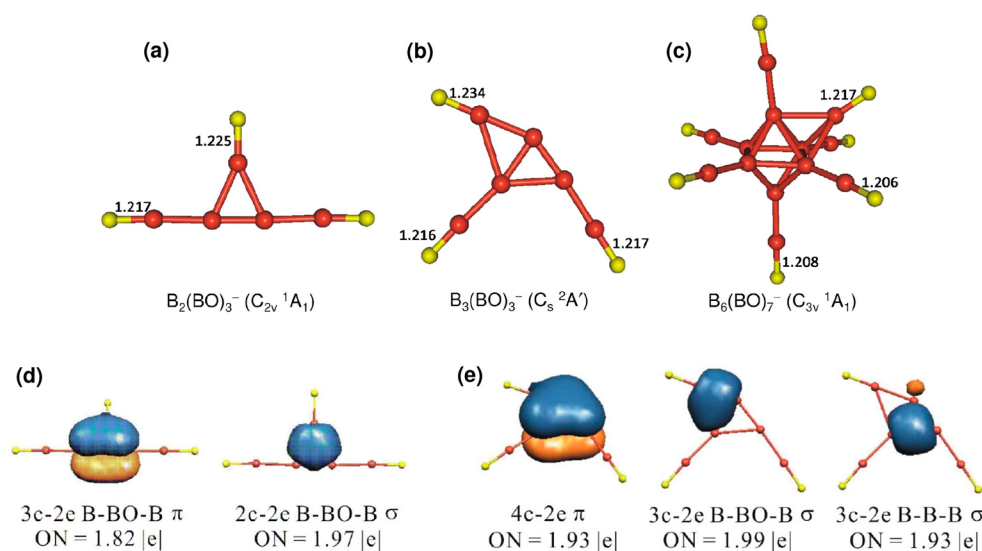


**Figure 10.** Optimized global-minimum structures for (a)  $B_2(BO)_3^-$  and (b)  $B_3(BO)_3^-$ , as well as (c) the structure of a model  $B_6(BO)_7^-$  cluster, at the B3LYP/aug-cc-pVTZ level. The delocalized bonding elements are revealed for (d)  $B_2(BO)_3^-$  and (e)  $B_3(BO)_3^-$  from the adaptive natural density partitioning (AdNDP) analyses. The  $B\equiv O$  bond distances (in Å) and occupation numbers (ONs) are labeled. Reproduced in part with permission from ref 37. Copyright 2011 Wiley. Panel c is modified from ref 38. Copyright 2013 American Chemical Society.

boronyl boroxine, rendering it a new member of the inorganic benzene family and a true analogue to boroxine and borazine. Despite its relatively small size, boronyl boroxine contains all critical structural and bonding elements in glassy bulk  $B_2O_3$  and high temperature  $B_2O_3$  liquids: the six-membered  $B_3O_3$  boroxol ring and the BO terminal groups. Thus, boronyl boroxine and similar larger clusters are valuable molecules to mimic the microscopic, short-range structures of amorphous  $B_2O_3$  glasses and liquids and to model their nucleation and growth. Synthesis and isolation of boronyl boroxine may also be a promising target to pursue.

## 6. ON THE $\pi$ AND $\sigma$ DOUBLE CONJUGATION IN BORON DIBORONYL CLUSTERS

A series of boron dioxide clusters were characterized recently in PES measurements, which are formulated as boron diboronyl complexes.<sup>39</sup> All  $B_n(BO)_2^-$  and  $B_n(BO)_2$  clusters adopt planar, elongated, double-chain nanoribbon structures, with two

terminal BO groups attached to the  $B_n$  core in either *trans* or *cis* fashion (Figure 11). The shapes are very different from bare  $B_n^-/B_n$  clusters,<sup>3–15</sup> where circular versus elongated structures occur alternatively as a function of size  $n$ . The ground-state ADEs of  $B_n(BO)_2^-$  ( $n = 4–12$ ), that is, the EAs of their neutrals, follow a regular  $4n$  pattern (Figure 12). Computational ground-state vertical detachment energies (VDEs) for  $B_nH_2^-$  show a similar trend.<sup>55,56</sup> Preliminary B3LYP calculations predicted that larger nanoribbon clusters,  $B_{16}(BO)_2$  and  $B_{20}(BO)_2$ , are also highly stable species and their anions and dianions appear to be even better defined energetically, thus extending the nanoribbon clusters to up to  $\sim 15$  Å in length. The greater potency for boron dioxide clusters to adopt nanoribbon structures relative to the  $B_nH_2^-/B_nH_2$  clusters<sup>55,56</sup> is likely due to both the polar nature and  $\pi$ -bonding capability of BO, which marks the limit of the BO/H isolobal analogy. The nanoribbon shape can effectively reduce Coulomb repulsion between two BO terminals at the two ends, and

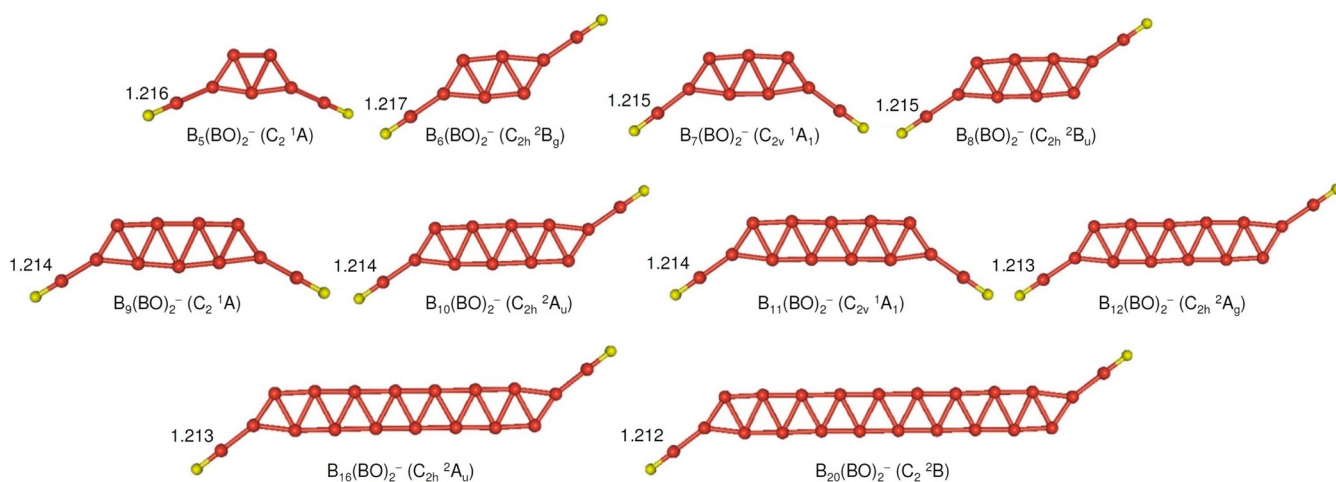


**Figure 11.** Optimized double-chain nanoribbon structures for  $B_n(\text{BO})_2^-$  ( $n = 5-12, 16, \text{ and } 20$ ) at the B3LYP/6-311++G(d,p) level. The  $\text{B}=\text{O}$  bond distances (in Å) are labeled. Reproduced with permission from ref 39. Copyright 2013 AIP Publishing.

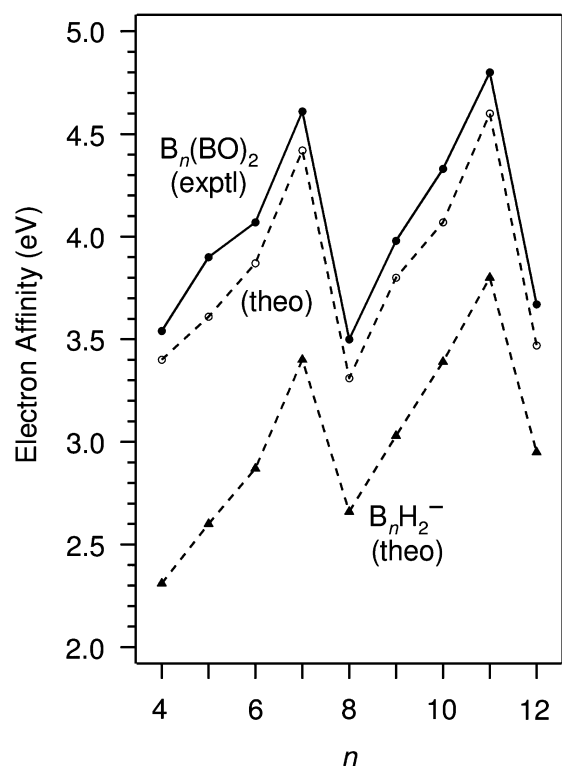


**Figure 12.** Experimental electron affinities (EAs) of  $B_n(\text{BO})_2$  ( $n = 4-12$ ; ●) as a function of  $n$ , compared with theoretical EAs at the single-point CCSD(T)//B3LYP/6-311++G(d,p) level (○). Computational ground-state vertical detachment energies of  $B_n\text{H}_2^-$  at the B3LYP level (filled triangles) are also shown for comparison. Reproduced with permission based on ref 39. Copyright 2013 AIP Publishing.

further elongates (and stabilizes) the  $\pi$  conjugation in the system. Note that the ultimate size and length for free-standing  $B_n(\text{BO})_2^{0/-/2-}$  nanoribbon clusters are still open.

There exist  $(n-2)/(n-1)/n$  delocalized electrons in a  $B_n(\text{BO})_2/B_n(\text{BO})_2^-/B_n(\text{BO})_2^{2-}$  cluster, respectively, which are coupled into either  $\pi$  or  $\sigma$  bonds between two B chains. The  $\pi$  and  $\sigma$  sets of orbitals are orthogonal to and independent of each other, sequencing according to their energies, where a  $\pi$  orbital appears slightly more stable than its  $\sigma$  counterpart, presumably due to better orbital overlapping.<sup>39</sup> This relatively rigid filling

leads to a regular  $\pi$  and  $\sigma$  alternation, reappearing every four B atoms, which underlies the  $4n$  pattern (Figure 12). AdNDP analyses are summarized in Figure 13. With the formation of  $\pi$  conjugation between the delocalized  $\pi$  MOs, these nanoribbon clusters are boronyl analogues of the conjugated *polyenes*, where a rhombic  $B_4$  unit is equivalent to a  $\text{C}=\text{C}$  unit in polyenes. Furthermore, the delocalized  $\sigma$  framework closely parallels the  $\pi$  framework, making it imperative to introduce the concept of  $\sigma$  conjugation to the system as well. There has been no  $\sigma$  conjugation ever observed in organic hydrocarbons. Thus, the  $\pi$  and  $\sigma$  double conjugation in  $B_n(\text{BO})_2^-/B_n(\text{BO})_2$  clusters,<sup>39</sup> which is apparently also true (but was not recognized previously) for  $B_n\text{H}_2^-/B_n\text{H}_2$ ,<sup>55,56</sup> makes these boron-based nanoribbon clusters unique species.

Depending on the size  $n$  and charge state of a nanoribbon cluster, the effective distribution of  $\pi$  or  $\sigma$  clouds alters (Figure 13). In the ideal cases, such as  $B_8(\text{BO})_2$ ,  $B_{12}(\text{BO})_2$ ,  $B_{16}(\text{BO})_2$ , and  $B_{20}(\text{BO})_2$ , which have one more  $\pi$  orbital than  $\sigma$  orbitals, the electron clouds exhibit a strict spatial  $\pi$  versus  $\sigma$  alternation (category 1). This pattern makes each segment of the nanoribbon more or less evenly bonded, analogous to carbon chains in the *cumulenes*. Very recently, a concept of ribbon aromaticity<sup>57</sup> is proposed to account for such “magic” clusters. Ribbon aromaticity follows the electron counting of  $2(n+1)\pi + 2n\sigma$ , that is,  $(4n+2)$ , which is exactly the Hückel rule.

When the number of  $\pi$  orbitals is equal to the number of  $\sigma$  orbitals, the  $\pi$  and  $\sigma$  clouds can overlap exactly (category 2), as exemplified by  $B_6(\text{BO})_2$  and  $B_{10}(\text{BO})_2$ . This introduces more bonded versus less bonded segments along the nanoribbon, which differ by two bonds per  $B_4$  unit, rendering them even closer analogues of the conjugated *polyynes*. For example,  $B_4(\text{BO})_2^{2-}$  (ref 39) and  $B_6(\text{BO})_2$  are boronyl analogues of acetylene ( $\text{C}_2\text{H}_2$ ), while  $B_{10}(\text{BO})_2$  is similar to butadiyne ( $\text{C}_4\text{H}_2$ ).

In between the above extremes lies category 3, which features partial overlap of  $\pi$  and  $\sigma$  clouds. In such cases, the nanoribbon is segmented into “triangles” that are covered by dual  $\pi$  and  $\sigma$  clouds,  $\pi$  or  $\sigma$  clouds only, or neither. In short, owing to the  $\pi$  and  $\sigma$  double conjugation, boron dioxide nanoribbon clusters offer a rich variety of inorganic analogues of *polyenes*, *cumulenes*, and *polyynes*. Interestingly, upon changing the charge state, a specific cluster can switch between the categories, offering



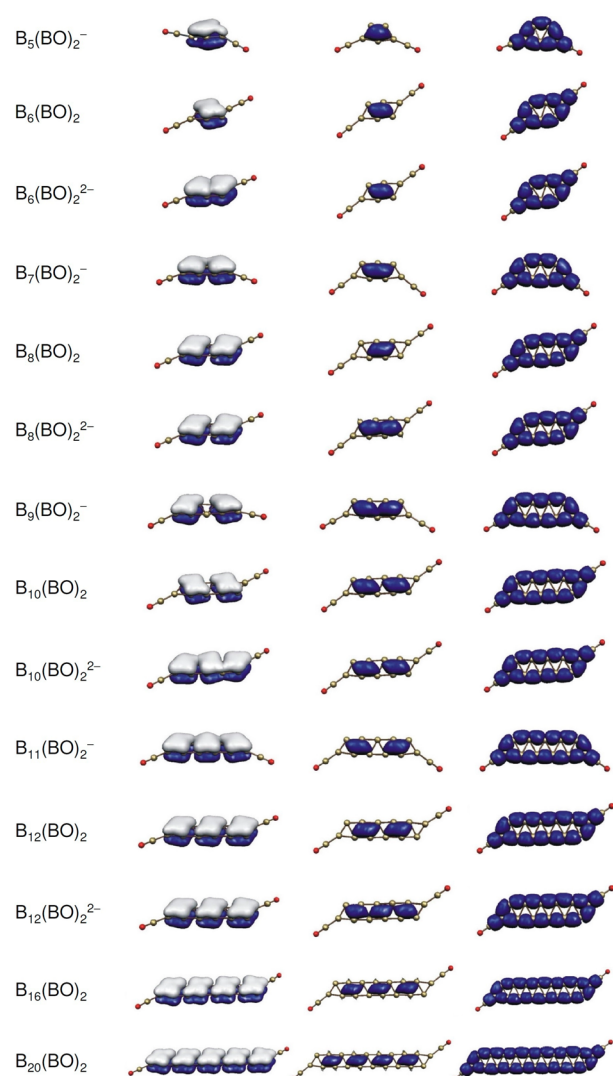


**Figure 13.** Double ( $\pi$  and  $\sigma$ ) conjugation for  $B_n(\text{BO})_2$ ,  $B_n(\text{BO})_2^-$ , and  $B_n(\text{BO})_2^{2-}$  ( $n = 5-12, 16$ , and  $20$ ) as revealed from the adaptive natural density partitioning (AdNDP) analyses. Left column,  $\pi$  clouds; middle,  $\sigma$  clouds; right, two-center two-electron B–B and B–(BO)  $\sigma$  bonds. The localized bonding elements within the BO groups (B $\equiv$ O triple bond, O 2s lone pair) are not shown. Reproduced with permission from ref 39. Copyright 2013 AIP Publishing.

opportunities to tailor the electronic properties via charging or with different ligands.

Note that the electron clouds (either  $\pi$  or  $\sigma$ ) are primarily islanded on the rhombic  $B_4$  units as  $4c-2e$  bonds, well supporting the  $4n$  pattern observed in the electron binding energies (Figure 12), which reinforces the notion of  $B_4$  as the optimal structural block in the nanoribbon clusters. Lastly, double-chain nanoribbon boron structures are found to be the key structural elements in low-dimensional boron nanostructures, such as the tubular boron clusters, boron fullerenes, boron nanotubes, and monolayer boron sheets.

## 7. CONCLUSIONS AND PERSPECTIVE

This Account provides a brief overview of the recent developments in boronyl chemistry, which span from gas-phase boronyl clusters to the first synthetic platinum boronyl compound. In all species, the BO group maintains its structural and chemical integrity. These results have firmly established

boronyl as a new inorganic ligand. Boronyl chemistry is an emerging field, offering opportunities to develop new chemistry in parallel to that of CN. Among further research directions, the synthesis and characterization of new transition metal boronyl clusters in the gas phase should represent a fertile ground. Bulk synthesis of new metal boronyl compounds and studies of their reactivity and catalysis are also of interest. The nature of the interaction between a metal center and a boronyl group, in particular whether and how BO acts as a  $\pi$  acceptor in the metal boronyls, remains to be elucidated. In the boron oxide clusters, fine-tuning the B versus O compositions should result in further structural diversity, which may serve as molecular models for mechanistic understanding of the combustion of boron and boranes. Boronyl is also expected to play a role in oxygen-rich boron oxides, which are basically unknown to date. For metal boronyls, carbon boronyls, and boron boronyls, the coordination chemistry beyond the terminal and  $\eta^2$  bridging BO ligands also offers vast opportunities, in light of the isolobal relationship between BO/BO $^-$  and CN/CN $^-$  or CO and the rich coordination chemistry of CN and CO. Furthermore, with regard to the formation of complexes with multiple boronyl groups, it remains to be explored whether the BO radical is prone to oligomerization. For the boronyl species discussed in this Account, oligomerization does not seem to play a role, presumably because BO is a polar molecule and intramolecular Coulomb repulsion between the BO groups dominates the structures of the complexes. Indeed, the BO groups tend to situate themselves as far apart as possible in all these boronyl complexes.

## ■ AUTHOR INFORMATION

### Corresponding Authors

\*E-mail: hj.zhai@sxu.edu.cn.

\*E-mail: lisidian@sxu.edu.cn.

\*E-mail: lai-sheng\_wang@brown.edu.

### Funding

This work was supported by the US National Science Foundation (Grant CHE-1263745) and the National Natural Science Foundation of China (Grant Nos. 21243004 and 21373130). H.J.Z. gratefully acknowledges the start-up fund from Shanxi University for support.

### Notes

The authors declare no competing financial interest.

### Biographies

**Hua-Jin Zhai** is a distinguished professor in the Institute of Molecular Science, Shanxi University. He studied physics at Wuhan University (B.S. 1990) and the Chinese Academy of Sciences (Ph.D. 1998) and conducted postdoctoral research in physical chemistry at Washington State University and Pacific Northwest National Laboratory (WSU/PNNL). He was formerly a research scientist at WSU/PNNL and a senior research scientist at Brown University. Professor Zhai's research interests are centered in cluster physics, experimental physical chemistry, and computational chemistry.

**Qiang Chen** received his B.S. from the department of chemistry at Xinzhou Teachers' University in 2008. He is currently pursuing his Ph.D. under Professor Si-Dian Li at Shanxi University. His thesis research focuses on the structures and bonding of boron-rich binary clusters and the design of all-boron graphene-like materials.

**Hui Bai** received her B.S. from the department of chemistry at Xinzhou Teachers' University in 2009. She is currently pursuing her

Ph.D. under Professor Si-Dian Li at Shanxi University. Her thesis research focuses on the structures and properties of novel boron-rich boron hydride clusters and boron-based nanomaterials.

**Si-Dian Li** is a professor in the Institute of Molecular Science, Shanxi University. He received his B.S. from Beijing Normal University, M.S. from Shanxi University, and Doctor of Engineering from Xi'an Jiaotong University. He has carried out cooperative research at Sussex University in the U.K. and Pacific Northwest National Laboratory in the United States. Professor Li's fields of interest include theoretical and experimental research in structural chemistry, materials chemistry, and computational chemistry.

**Lai-Sheng Wang** received his B.S. degree in chemistry from Wuhan University in China and his Ph.D. in physical chemistry from the University of California at Berkeley. After a postdoctoral stay at Rice University, he took a joint position between Washington State University and Pacific Northwest National Laboratory and then accepted an appointment as Professor of Chemistry at Brown University in 2009. His research group focuses on the investigation of the size-dependent properties of nanoclusters using photoelectron spectroscopy and computational tools, as well as spectroscopic studies of free multiply charged anions and complex solution-phase molecules using electrospray ionization and photodetachment spectroscopy. His group has developed cryogenic ion traps to create cold anions from electrospray for high-resolution spectroscopic studies. Recently, his lab has also ventured into bulk syntheses of atom-precise and ligand-protected gold nanoclusters.

## REFERENCES

- Albert, B.; Hillebrecht, H. Boron: Elementary challenge for experimenters and theoreticians. *Angew. Chem., Int. Ed.* **2009**, *48*, 8640–8668.
- Lipscomb, W. N. The boranes and their relatives. *Science* **1977**, *196*, 1047–1055.
- Zhai, H. J.; Alexandrova, A. N.; Birch, K. A.; Boldyrev, A. I.; Wang, L. S. Hepta- and octacoordinate boron in molecular wheels of eight- and nine-atom boron clusters: Observation and confirmation. *Angew. Chem., Int. Ed.* **2003**, *42*, 6004–6008.
- Zhai, H. J.; Kiran, B.; Li, J.; Wang, L. S. Hydrocarbon analogues of boron clusters – Planarity, aromaticity and antiaromaticity. *Nat. Mater.* **2003**, *2*, 827–833.
- Kiran, B.; Bulusu, S.; Zhai, H. J.; Yoo, S.; Zeng, X. C.; Wang, L. S. Planar-to-tubular structural transition in boron clusters:  $B_{20}$  as the embryo of single-walled boron nanotubes. *Proc. Natl. Acad. Sci. U.S.A.* **2005**, *102*, 961–964.
- Sergeeva, A. P.; Zubarev, D. Yu.; Zhai, H. J.; Boldyrev, A. I.; Wang, L. S. A photoelectron spectroscopic and theoretical study of  $B_{16}^-$  and  $B_{16}^{2-}$ : An all-boron naphthalene. *J. Am. Chem. Soc.* **2008**, *130*, 7244–7246.
- Huang, W.; Sergeeva, A. P.; Zhai, H. J.; Averkiev, B. B.; Wang, L. S.; Boldyrev, A. I. A concentric planar doubly  $\pi$ -aromatic  $B_{19}^-$  cluster. *Nat. Chem.* **2010**, *2*, 202–206.
- Sergeeva, A. P.; Averkiev, B. B.; Zhai, H. J.; Boldyrev, A. I.; Wang, L. S. All-boron analogues of aromatic hydrocarbons:  $B_{17}^-$  and  $B_{18}^-$ . *J. Chem. Phys.* **2011**, *134*, No. 224304, (11 pages).
- Piazza, Z. A.; Li, W. L.; Romanescu, C.; Sergeeva, A. P.; Wang, L. S.; Boldyrev, A. I. A photoelectron spectroscopy and *ab initio* study of  $B_{21}^-$ : Negatively charged boron clusters continue to be planar at 21. *J. Chem. Phys.* **2012**, *136*, No. 104310, (9 pages).
- Sergeeva, A. P.; Piazza, Z. A.; Romanescu, C.; Li, W. L.; Boldyrev, A. I.; Wang, L. S.  $B_{22}^-$  and  $B_{23}^-$ : All-boron analogues of anthracene and phenanthrene. *J. Am. Chem. Soc.* **2012**, *134*, 18065–18073.
- Piazza, Z. A.; Hu, H. S.; Li, W. L.; Zhao, Y. F.; Li, J.; Wang, L. S. Planar hexagonal  $B_{36}$  as a potential basis for extended single-atom layer boron sheets. *Nat. Commun.* **2014**, *5*, No. 3113, (6 pages).
- Oger, E.; Crawford, N. R. M.; Kelting, R.; Weis, P.; Kappes, M. M.; Ahlrichs, R. Boron cluster cations: Transition from planar to cylindrical structures. *Angew. Chem., Int. Ed.* **2007**, *46*, 8503–8506.
- Fowler, J. E.; Ugalde, J. M. The curiously stable  $B_{13}^+$  cluster and its neutral and anionic counterparts: The advantages of planarity. *J. Phys. Chem. A* **2000**, *104*, 397–403.
- Aihara, J. I.; Kanno, H.; Ishida, T. Aromaticity of planar boron clusters confirmed. *J. Am. Chem. Soc.* **2005**, *127*, 13324–13330.
- Alexandrova, A. N.; Boldyrev, A. I.; Zhai, H. J.; Wang, L. S. All-boron aromatic clusters as potential new inorganic ligands and building blocks in chemistry. *Coord. Chem. Rev.* **2006**, *250*, 2811–2866.
- Bauer, S. H. Oxidation of B, BH,  $BH_2$ , and  $B_nH_n$  species: Thermochemistry and kinetics. *Chem. Rev.* **1996**, *96*, 1907–1916.
- Wenthold, P. G.; Kim, J. B.; Jonas, K. L.; Lineberger, W. C. An experimental and computational study of the electron affinity of boron oxide. *J. Phys. Chem. A* **1997**, *101*, 4472–4474.
- Zhai, H. J.; Wang, L. M.; Li, S. D.; Wang, L. S. Vibrationally-resolved photoelectron spectroscopy of  $BO^-$  and  $BO_2^-$ : A joint experimental and theoretical study. *J. Phys. Chem. A* **2007**, *111*, 1030–1035.
- Kinney, C. R.; Pontz, D. F. Boranilide. *J. Am. Chem. Soc.* **1935**, *57*, 1128–1129.
- Mackenzie, J. D. Structure of liquid boron trioxide. *J. Phys. Chem.* **1959**, *63*, 1875–1878.
- Doyle, R. J. High molecular weight boron oxides in the gas phase. *J. Am. Chem. Soc.* **1988**, *110*, 4120–4126.
- Bock, H.; Cederbaum, L.; von Niessen, W.; Paetzold, P.; Rosmus, P.; Solouki, B. Methylboron oxide,  $H_3C-B\equiv O$ . *Angew. Chem., Int. Ed. Engl.* **1989**, *28*, 88–90.
- Wang, L. S.; Cheng, H. S.; Fan, J. Photoelectron spectroscopy of size-selected transition metal clusters:  $Fe_n^-$ ,  $n = 3-24$ . *J. Chem. Phys.* **1995**, *102*, 9480–9493.
- Zubarev, D. Yu.; Boldyrev, A. I.; Li, J.; Zhai, H. J.; Wang, L. S. On the chemical bonding of gold in auro-boron oxide clusters  $Au_nBO^-$  ( $n = 1-3$ ). *J. Phys. Chem. A* **2007**, *111*, 1648–1658.
- Miao, C. Q.; Lu, H. G.; Li, S. D. Covalent bonding in  $Au(BO)_2^-$  and  $Au(BS)_2^-$ . *J. Cluster Sci.* **2013**, *24*, 233–241.
- Zhou, M.; Jiang, L.; Xu, Q. C–C double- and triple-bond formation from reactions of B atoms with CO: Experimental and theoretical characterization of OBCCO and OBCCBO molecules in solid argon. *Chem.—Eur. J.* **2004**, *10*, 5817–5822.
- Li, S. D.; Miao, C. Q.; Guo, J. C.; Ren, G. M. Carbon boronyls: Species with higher viable possibility than boron carbonyls at the density functional theory. *J. Comput. Chem.* **2005**, *26*, 799–802.
- Li, S. D.; Guo, J. C.; Ren, G. M. Density functional theory investigations on boronyl-substituted ethylenes  $C_2H_{4-m}(BO)_m$  ( $m = 1-4$ ) and acetylenes  $C_2H_{2-m}(BO)_m$  ( $m = 1, 2$ ). *THEOCHEM* **2007**, *821*, 153–159.
- Miao, C. Q.; Li, S. D.  $B_n(BO)_n^{2-}$ ,  $CB_{n-1}(BO)_n^-$ , and  $C_2B_{n-2}(BO)_n$  ( $n = 5-12$ ): Cage-like boron oxide clusters analogous to *closo*- $B_nH_n^{2-}$ ,  $CB_{n-1}H_n^-$ , and  $C_2B_{n-2}H_n$ . *Sci. China Chem.* **2011**, *54*, 756–761.
- McAnoy, A. M.; Dua, S.; Schroder, D.; Bowie, J. H.; Schwarz, H. The formation of CCBO and  $[CCBO]^+$  from  $[CCBO]^-$  in the gas phase: A joint experimental and theoretical study. *J. Phys. Chem. A* **2003**, *107*, 1181–1187.
- McAnoy, A. M.; Dua, S.; Schroder, D.; Bowie, J. H.; Schwarz, H. Generation of neutral CCCCBO in the gas phase from  $[CCCCBO]^-$  and rearrangement of energized CCCCBO to OCCCCB: A joint experimental and theoretical investigation. *J. Phys. Chem. A* **2004**, *108*, 2426–2430.
- Zhai, H. J.; Li, S. D.; Wang, L. S. Boronyls as key structural units in boron oxide clusters:  $B(BO)_2^-$  and  $B(BO)_3^-$ . *J. Am. Chem. Soc.* **2007**, *129*, 9254–9255.
- Li, S. D.; Zhai, H. J.; Wang, L. S.  $B_2(BO)_2^{2-}$  – Diboronyl diborene: A linear molecule with a triple boron-boron bond. *J. Am. Chem. Soc.* **2008**, *130*, 2573–2579.

(34) Zhai, H. J.; Miao, C. Q.; Li, S. D.; Wang, L. S. On the analogy of B-BO and B-Au chemical bonding in the  $B_{11}O^-$  and  $B_{10}Au^-$  clusters. *J. Phys. Chem. A* **2010**, *114*, 12155–12161.

(35) Chen, Q.; Zhai, H. J.; Li, S. D.; Wang, L. S. Probing the structures and chemical bonding of boron-boronyl clusters using photoelectron spectroscopy and computational chemistry:  $B_n(BO)_n^-$  ( $n = 1-3$ ). *J. Chem. Phys.* **2012**, *137*, No. 044307, (7 pages).

(36) Bai, H.; Zhai, H. J.; Li, S. D.; Wang, L. S. Photoelectron spectroscopy of aromatic compound clusters of the  $B_{12}$  all-boron benzene:  $B_{12}Au^-$  and  $B_{12}(BO)^-$ . *Phys. Chem. Chem. Phys.* **2013**, *15*, 9646–9653.

(37) Zhai, H. J.; Guo, J. C.; Li, S. D.; Wang, L. S. Bridging  $\eta^2$ -BO in  $B_2(BO)_3^-$  and  $B_3(BO)_3^-$  clusters: Boronyl analogs of boranes. *ChemPhysChem* **2011**, *12*, 2549–2553.

(38) Guo, J. C.; Lu, H. G.; Zhai, H. J.; Li, S. D. Face-capping  $\mu^3$ -BO in  $B_6(BO)_7^-$ : Boron oxide analogue of  $B_6H_7^-$  with rhombic 4c–2e bonds. *J. Phys. Chem. A* **2013**, *117*, 11587–11591.

(39) Zhai, H. J.; Chen, Q.; Bai, H.; Lu, H. G.; Li, W. L.; Li, S. D.; Wang, L. S. Pi and sigma double conjugations in boronyl polyboronene nanoribbons:  $B_n(BO)_2^-$  and  $B_n(BO)_2$  ( $n = 5-12$ ). *J. Chem. Phys.* **2013**, *139*, No. 174301, (7 pages).

(40) Yao, W. Z.; Guo, J. C.; Lu, H. G.; Li, S. D.  $T_d$   $B(BO)_4^-$ : A tetrahedral boron oxide cluster analogous to boron hydride  $T_d$   $BH_4^-$ . *J. Phys. Chem. A* **2009**, *113*, 2561–2564.

(41) Drummond, M. L.; Meunier, V.; Sumpter, B. G. Structure and stability of small boron and boron oxide clusters. *J. Phys. Chem. A* **2007**, *111*, 6539–6551.

(42) Tai, T. B.; Nguyen, M. T. Structure and electron delocalization of the boron oxide cluster  $B_3(BO)_3$  and its anion and dianion. *Chem. Phys. Lett.* **2009**, *483*, 35–42.

(43) Nguyen, M. T.; Matus, M. H.; Ngan, V. T.; Grant, D. J.; Dixon, D. A. Thermochemistry and electronic structure of small boron and boron oxide clusters and their anions. *J. Phys. Chem. A* **2009**, *113*, 4895–4909.

(44) Tai, T. B.; Nguyen, M. T.; Dixon, D. A. Thermochemical properties and electronic structure of boron oxides  $B_nO_m$  ( $n = 5-10$ ,  $m = 1-2$ ) and their anions. *J. Phys. Chem. A* **2010**, *114*, 2893–2912.

(45) Burkholder, T. R.; Andrews, L. Reactions of boron atoms with molecular oxygen. Infrared spectra of BO,  $BO_2$ ,  $B_2O_2$ ,  $B_2O_3$ , and  $BO_2^-$  in solid argon. *J. Chem. Phys.* **1991**, *95*, 8697–8709.

(46) Li, D. Z.; Bai, H.; Chen, Q.; Lu, H. G.; Zhai, H. J.; Li, S. D. Perfectly planar boronyl boroxine  $D_{3h}$   $B_6O_6$ : A boron oxide analog of boroxine and benzene. *J. Chem. Phys.* **2013**, *138*, No. 244304, (8 pages).

(47) Braunschweig, H.; Radacki, K.; Schneider, A. Oxoboryl complexes: Boron-oxygen triple bonds stabilized in the coordination sphere of platinum. *Science* **2010**, *328*, 345–347.

(48) Häkkinen, H.; Yoon, B.; Landman, U.; Li, X.; Zhai, H. J.; Wang, L. S. On the electronic and atomic structures of small  $Au_n^-$  ( $n = 4-14$ ) clusters: A photoelectron spectroscopy and density-functional study. *J. Phys. Chem. A* **2003**, *107*, 6168–6175.

(49) Zhai, H. J.; Wang, L. S.; Zubarev, D. Yu.; Boldyrev, A. I. Gold apes hydrogen. The structure and bonding in the planar  $B_7Au_2^-$  and  $B_7Au_2$  clusters. *J. Phys. Chem. A* **2006**, *110*, 1689–1693.

(50) Zhou, M.; Tsumori, N.; Li, Z.; Fan, K.; Andrews, L.; Xu, Q. OCBCO: A neutral molecule with some boron-boron triple bond character. *J. Am. Chem. Soc.* **2002**, *124*, 12936–12937.

(51) Wu, H. S.; Jiao, H.; Wang, Z. X.; Schleyer, P. v. R. Monocyclic boron carbonyls: Novel aromatic compounds. *J. Am. Chem. Soc.* **2003**, *125*, 4428–4429.

(52) Zubarev, D. Yu.; Boldyrev, A. I. Developing paradigms of chemical bonding: Adaptive natural density partitioning. *Phys. Chem. Chem. Phys.* **2008**, *10*, 5207–5217.

(53) Braunschweig, H.; Dewhurst, R. D.; Hammond, K.; Mies, J.; Radacki, K.; Vargas, A. Ambient-temperature isolation of a compound with a boron-boron triple bond. *Science* **2012**, *336*, 1420–1422.

(54) Chen, Q.; Lu, H. G.; Zhai, H. J.; Li, S. D. Chemical bonding in electron-deficient boron oxide clusters: Core boronyl groups, dual 3c–

4e hypervalent bonds, and rhombic 4c–4e bonds. *Phys. Chem. Chem. Phys.* **2014**, *16*, 7274–7279.

(55) Li, W. L.; Romanescu, C.; Jian, T.; Wang, L. S. Elongation of planar boron clusters by hydrogenation: Boron analogues of polyenes. *J. Am. Chem. Soc.* **2012**, *134*, 13228–13231.

(56) Li, D. Z.; Chen, Q.; Wu, Y. B.; Lu, H. G.; Li, S. D. Double-chain planar  $D_{2h}$   $B_4H_2$ ,  $C_{2h}$   $B_8H_2$ , and  $C_{2h}$   $B_{12}H_2$ : Conjugated aromatic borennes. *Phys. Chem. Chem. Phys.* **2012**, *14*, 14769–14774.

(57) Bai, H.; Chen, Q.; Miao, C. Q.; Mu, Y. W.; Wu, Y. B.; Lu, H. G.; Zhai, H. J.; Li, S. D. Ribbon aromaticity in double-chain planar  $B_nH_2^{2-}$  and  $Li_2B_nH_2$  nanoribbon clusters up to  $n = 22$ : Lithiated boron dihydride analogues of polyenes. *Phys. Chem. Chem. Phys.* **2013**, *15*, 18872–18880.